ECS Transactions, 11 (1) 683-692 (2007)
10.1149/1.2780981 ©The Electrochemical Society

Capillary Pressure-Saturation Behavior of Carbon Paper Fuel Cell Diffusion Media: A Validated Approach

E. C. Kumbur [a,b] , K. V. Sharp[b], and M. M. Mench [a,*]

[a] Fuel Cell Dynamics and Diagnostics Laboratory
[b] Microscale Flow Laboratory
[*] Corresponding Author (mmm124@psu.edu)

Department of Mechanical and Nuclear Engineering,
The Pennsylvania State University, University Park, PA 16802, USA

This study is motivated by the need to develop a validated capillary pressure-saturation relationship that can precisely describe the capillary transport characteristics of the fuel cell diffusion media (DM). A series of capillary pressure-saturation measurements were performed for SGL 24 series DMs tailored with various degrees of PTFE loadings (from 5% to 20% of *wt*.) over a wide range of operating conditions (*i.e*. at different temperatures and compressions). The benchmark data were then utilized to deduce an appropriate form of Leverett approach that can precisely determine the capillary pressure of the tested fuel cell DMs as a function of hydrophobic additive content, operating temperature, liquid saturation, compression pressure and uncompressed porosity of the DM.

Introduction

Proper engineering of fuel cell materials is of utmost importance for attaining the optimized water balance required to achieve high cell performance, enhanced durability, and frozen shutdown/start-up capability. Among the fuel cell components, the fuel cell diffusion media (DM) represents the key component as it governs the water transport mechanism inside the porous electrodes of PEFCs [1]. The fuel cell DM is typically made of carbon-fiber based products, such as non-woven carbon paper and woven cloth, having a non-uniform pore distribution [2,3]. Because of the hydrophilic nature of these randomly packed carbon fibers, the DM substrates are impregnated with the anisotropic coating of PTFE, thereby yielding mixed wettability characteristics.

The inherent complexity of liquid/gas flow and the marked heterogeneity of the thin-film fuel cell DM limit the benchmarking of these porous materials. Due to the scarcity of experimental data, to date modeling has come to the forefront as a major approach to characterize the complex interaction between the DM transport properties and the performance of a fuel cell. Almost every multi-phase transport model requires the specific capillary pressure-saturation relationship of fluid and porous medium to correlate the capillary pressure as a function of saturation, wettability and other material properties. In most fuel cell models [4], the common approach to simulate the capillary transport in these porous materials relies on the semi-empirical correlation proposed by Leverett [5] and Udell [14]. Even though the classical Leverett approach, indeed, serves as a useful starting point to model the liquid transport in the porous DM, the specific concerns center around the morphological differences of the fuel cell DM and the conditions under which

the commonly used form of Leverett approach was derived. The standard Leverett approach equipped with *J*-function was originally derived to simulate a range of common soils that have *uniform wettability*, high length scales and high surface to volume ratios [2], whereas the thin structure and heterogeneous composition of the porous DM represents a new class of materials, and has not been fully treated in soil science. Hence, the direct application of this empirical relationship without true validation limits the effectiveness of models and hinders providing reliable guidance for the design of next generation fuel cell materials [2,6]. Therefore, the proper representation of capillary pressure-saturation relationship of a fuel cell DM is of high priority to accurately characterize the capillary transport inside the DM and improve the quality of the fuel cell models.

This study is motivated by the need to develop a more appropriate form of capillary pressure-saturation relationship that can precisely represent the capillary transport characteristics of the fuel cell DM. A validated capillary pressure-saturation empirical correlation is deduced from a wide range of capillary pressure-saturation measurements of the commercially available SGL 24 series DMs treated with various degrees of PTFE loadings (from 5% to 20% of wt.) at different temperatures (20, 50 and 80 °C) and under various compressions (0, 0.6 and 1.4 MPa) [7-9]. The present approach accurately determines the capillary pressure of the DM as a function of saturation, PTFE loading, DM material properties, compression and temperature.

Experimental

In the present study, SGL 24 series (SIGRACET®) carbon paper DMs, namely SGL 24BC (5% PTFE), SGL 24CC (10% PTFE) and SGL 24DC (20% PTFE) were utilized for benchmarking. The same types of DMs have been selected in order to eliminate any possible uncertainties associated with the fabrication processes of these materials. The tested DM samples are treated with PTFE (hydrophobic agent) from 0 to 20% of total *wt*., which is in a typical hydrophobic treatment range preferred in conventional fuel cell applications. The base macro-porous substrate of the tested DM samples is coated with a 50 μm thick micro-porous layer (MPL).

A new technique called “Method of Standard Porosimetry (MSP)” developed by Porotech Ltd. was employed to measure the desired transport parameters such as capillary pressure, saturation, hydrophobic and hydrophilic porosity distribution. The operating principle of MSP technique is explained in [10]. The present experiments were performed at different temperatures, *i.e*., 20, 50 and 80 °C under fixed levels of compression, *i.e*., 0, 0.6 and 1.4 MPa in order to probe the changes in the morphological and the transport properties of the DM samples as a function of operating conditions. Additional compressive strain-stress experiments were also performed using a highly sensitive compression gauge to provide benchmark data on the elasticity behavior of the tested DM samples.

Results and Discussions

Based on the generated benchmark data, the detailed investigation of the capillary transport mechanism inside the DM has been performed. The effects of operating conditions and DM material properties on the morphological and transport characteristics of the DM were elucidated in depth. The major findings have been documented in a series of publications [7-9]. In this brief note, the main focus is placed on the

development of the appropriate capillary pressure-saturation correlation for the tested fuel cell DMs.

Total Pore Network Capillary Pressure-Saturation Curves

The drainage air/water capillary pressure-saturation curves for the chosen DM samples were measured at different temperatures (20, 50 and 80 °C) under various compressions (0, 0.6 and 1.4 MPa). The corresponding change in capillary pressure as a function of PTFE loading of the DM, the compression pressure and the operating temperature were quantified. The major findings are briefly summarized as follows.

Effect of Hydrophobicity: The air-water capillary pressure versus non-wetting phase saturation of the tested SGL 24 series DM samples is shown in Fig. 1. The individual curves follow similar trends; however, due to the different PTFE contents, the measured capillary pressure values differ slightly over the entire liquid saturation spectrum. Three distinctive saturation regions are observed in the capillary pressure-saturation curves. At low saturations (s_{nw}<0.4), the difference in measured capillary pressures between each DM is more pronounced. However, the discrepancy gradually diminishes as the saturation moves towards to the moderate saturation region (0.4<s_{nw}<0.7). In the high saturation region (s_{nw}>0.7), the discrepancy between the three tested DM samples increases noticeably again. The highest capillary pressure is observed in SGL 24DC treated with 20% PTFE, whereas the lowest value at a given saturation is observed in SGL 24BC treated with 5% PTFE. This behavior can be attributed to the strong dependence of capillary pressure on the hydrophobicity of the pore matrix. Physically, at pore level, rendering the carbon fiber more hydrophobic distorts the molecular force balance at the interface, forcing the liquid water to move towards an unstable state, which leads to a higher capillary pressure inside the pore. Therefore, any increase in PTFE loading facilities the water removal from the pores, leading to a considerable reduction in the water retention capacity (water storage) of the DM [7,11].

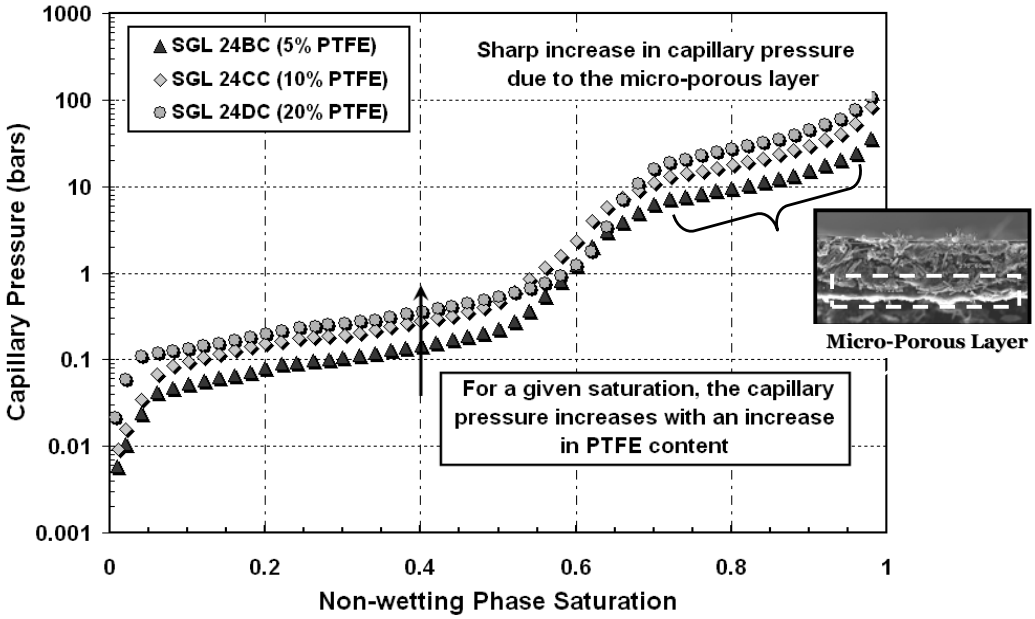

Figure 1: Measured capillary pressure versus non-wetting phase saturation of SGL 24 series carbon paper DMs at room temperature under no compression.

Effect of Compression: Figure 2 shows the non-wetting phase saturation versus air-water capillary pressure of SGL 24BC DM that is subjected to compression of 0, 0.6 and 1.4 MPa. The individual curves follow similar qualitative trends, yielding slightly different quantitative values. The capillary pressure appears to increase in parallel with compression within the compression range from 0 to 0.6 MPa. Physically, the compression generates strong local compressive-stresses, leading to a substantial reduction in the pore size. The decrease in pore size increases the surface energy (liquid water flow resistance) of the solid pore matrix. Therefore, a higher capillary pressure is required to overcome the increased surface energy of the distorted pores [8]. One interesting observation drawn from Fig. 2 is that any further increase in compression from 0.6 MPa seems to have less effect on the measured capillary pressure, which holds true for all tested DMs. This can be attributed to the relatively higher increase of the hydrophilic surface area of the DM substrate within this compression range. Any further increase in compression from 0.6 MPa seems to promote the dispersion of more hydrophilic sites, producing higher hydrophilic surface area, thus enhancing the hydrophilic characteristic of the DM. The decrease in the hydrophobicity of the DM with compression is also reported by Bayzlak *et al*. [15].

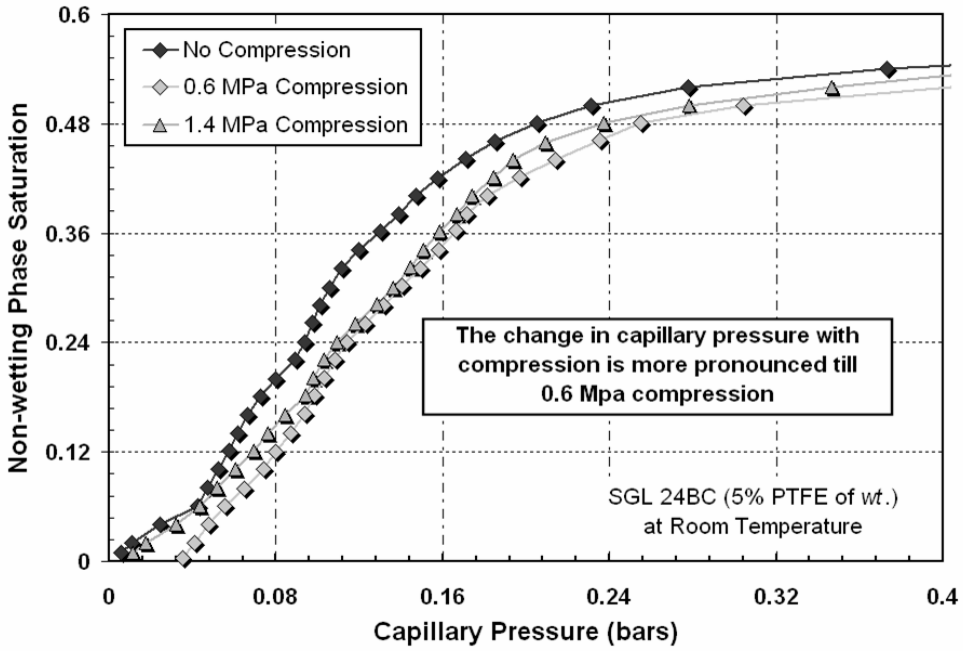

Figure 2: Measured capillary pressure versus non-wetting phase saturation of SGL 24BC DM sample under 0, 0.6 and 1.4 MPa compression.

Effect of Temperature: Figure 3 shows the measured capillary pressure-saturation curves of SGL 24BC, SGL 24CC and SGL 24DC at different temperatures. For a given non-wetting phase saturation, the capillary pressure is observed to decrease in response to the increase in temperature from 20 °C to 50 °C. This behavior is observed for SGL 24BC, SGL 24CC and to a certain extent for SGL 24DC carbon paper, since at high saturation region (s_{nw}>0.4), the temperature effect on the capillary pressure curves of SGL 24DC DM can not be clearly distinguished. As seen in Fig. 3, the capillary pressure measurements of SGL 24DC at both 20 °C and 50 °C appears to yield similar quantitative values in the region of s_{nw}>0.4, suggesting that the effect of temperature on the capillary pressure seems to be more pronounced for high PTFE coated DMs at low saturations

(s_{nw}<0.4) and low temperatures (~20°C). This can be potentially attributed to the higher dominance of wettability characteristics at low temperatures [9].

Physically, the temperature sensitivity of the capillary transport mechanism can not be explained through the concept of the surface tension alone. The pertinent studies [12,13] in soil science reveal that the interfacial tension and wettability characteristics are strongly coupled. Any increase in temperature influences the molecular interaction between the flowing fluids and solid pore matrix, which is followed by a subsequent increase in adhesion energy (sticking energy). In other words, the surface interaction between the phases and pore surface is greatly influenced by the temperature. Any increase in temperature is accompanied by an increase in the adhesion forces that reduce the surface tension and the intrinsic contact angle at the line of contact, which in turn, decreases the capillary pressure [9].

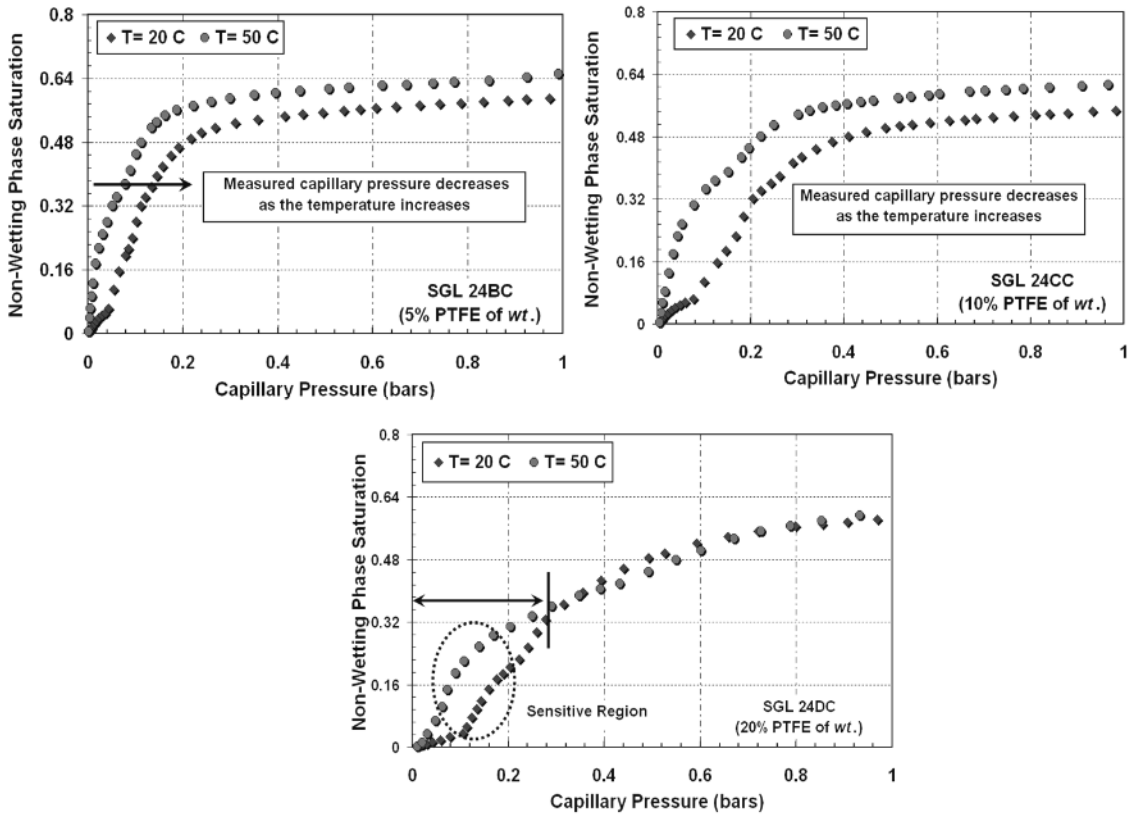

Figure 3: Measured capillary pressure versus non-wetting saturation for SGL 24BC, SGL 24CC and SGL 24DC DMs at 20 and 50 °C.

Empirical Correlation for Capillary Pressure-Saturation

To date, a semi-empirical approach proposed by Leverett [5] and Udell [14] (Eq. 1) has been commonly employed to represent the water transport or retention behavior of the fuel cell DM as a first step toward achieving an accurate two-phase transport model in fuel cells studies.

$$P_C = \gamma \cos\theta \cdot \left(\frac{\varepsilon}{k}\right)^{1/2} J(s_{nw})$$

$$J(s_{nw}) = \begin{cases} 1.417 \cdot (1 - s_{nw}) - 2.120 \cdot (1 - s_{nw})^2 + 1.263 \cdot (1 - s_{nw})^3 & \text{if } \theta < 90° \\ 1.417 \cdot s_{nw} - 2.120 \cdot s_{nw}{}^2 + 1.263 \cdot s_{nw}{}^3 & \text{if } \theta > 90° \end{cases} \quad [1]$$

where k, ε, θ and γ are permeability, porosity of the porous media, representative contact angle and surface tension, respectively. $J(s_{nw})$ represents the Leverett J-function derived from a common type of soil beds with uniform wettability. In a recent study by Kumbur et al. [2], the generic Leverett approach in its original form (Eq. 1) is found to be insufficient to describe the capillary transport characteristics of the porous DM with mixed wettability. The necessity of development of more appropriate form of Leverett approach is also emphasized in [2,6].

Based on this motivation, the generated capillary pressure-saturation benchmark data were complied in an expanded database to deduce an appropriate empirical correlation that accurately describes the capillary transport characteristics of the tested fuel cell DM samples. A multi-dimensional linear regression model was employed to precisely correlate the capillary pressure with the relevant non-dimensionelized experimental parameters. A total of 9600 experimental data points were processed and integrated into the computational database to determine the best polynomial fit. In order to improve the precision of the empirical correlation and eliminate the potential uncertainty associated with the complex shape of the capillary pressure-saturation curves, the overall saturation domain was divided into three regions as shown in Fig. 4, namely; $0<s_{nw}<0.50$ (less hydrophobic region), $0.50\leq s_{nw} \leq 0.65$ (transition region or relatively more hydrophobic region) and $0.65<s_{nw}<1.00$ (high capillary pressure region due to the existence of hydrophobic micro-porous layer).

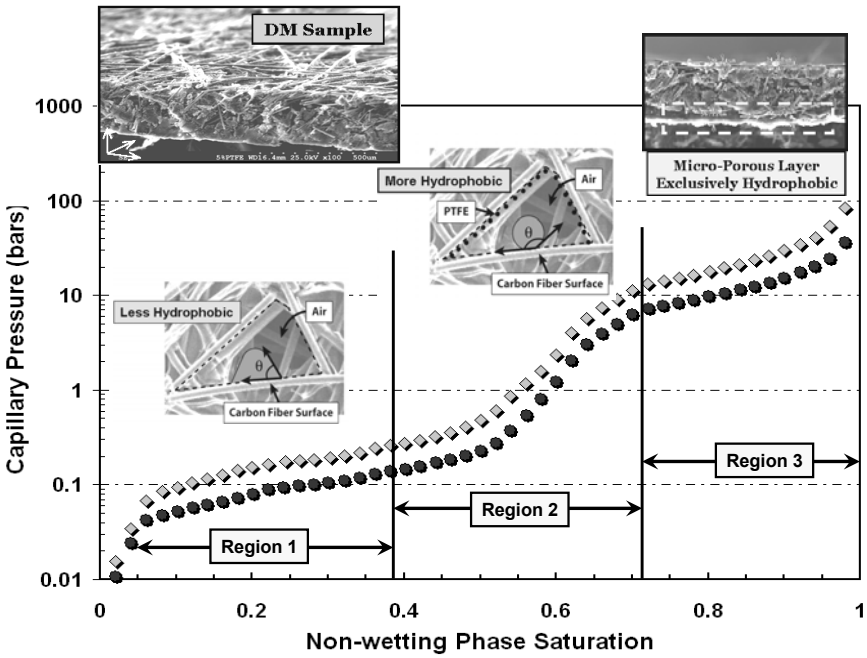

Figure 4: Schematic of three distinct regions observed in the measured capillary pressure-saturation curves of tested DM samples.

Our first effort was to implement the mixed wettability characteristics of the DM into *J* function given in Eq. 1. For that purpose, the benchmark data were categorized according the PTFE content of the DM for each operating conditions. Based on the specified saturation regions, the three continuous empirical fits (new Leverett-type function, $K(s_{nw})$) were generated and shown in Eq. 2. This function basically serves to account for the mixed wettability characteristics of the DM, which is not properly treated in original Leverett *J*-function. Adjusting the PTFE variable (*%wt.*) in the modified function, $K(s_{nw})$ (Eq. 2), enables successful determination of the capillary pressure as a function of hydrophobic additive loading of the DM. In addition, the variation in internal contact angle, a consequence of the mixed wettability characteristics of the DM, is implicitly embedded into the present Leverett-type function ($K(s_{nw})$), which in turn, eliminates the need for selection of a representative (unrealistic) surface contact angle.

$$K(s_{nw}) = \begin{cases} (\%wt.)\cdot\left[0.0469 - 0.00152\cdot(\%wt.) - 0.0406\cdot s_{nw}^{\ 2} + 0.143\cdot s_{nw}^{\ 3}\right] \\ +\,0.0561\cdot\ln s_{nw} \quad \text{for } 0 < s_{nw} \le 0.50 \\ (\%wt.)\cdot\left[1.534 - 0.0293\cdot(\%wt.) - 12.68\cdot s_{nw}^{\ 2} + 18.824\cdot s_{nw}^{\ 3}\right] \\ +\,3.416\cdot\ln s_{nw} \quad \text{for } 0.50 < s_{nw} \le 0.65 \\ (\%wt.)\cdot\left[1.7 - 0.0324\cdot(\%wt.) - 14.1\cdot s_{nw}^{\ 2} + 20.9\cdot s_{nw}^{\ 3}\right] \\ +\,3.79\cdot\ln s_{nw} \quad \text{for } 0.65 < s_{nw} < 1.00 \end{cases} \qquad [2]$$

where the parameters in $K(s_{nw})$ namely, (*% wt*) and s_{nw} are PTFE weight percentage of the DM and non-wetting liquid saturation, respectively.

In term of compression effect, additional stress-strain experiments were performed to capture the deformation and the change in effective porosity of SGL 24 series DM. Based on the elasticity behavior of the tested DM samples, the specific strain -compression pressure (*C*, MPa) relationship of the tested SGL 24 series DMs were obtained and shown in Eq. 3. It is worthwhile to emphasize that the compressive strain-stress relation given in Eq. 3 is a characteristic property of the SGL 24 series DMs and it varies for different DM materials. Based on the measured strain-stress behavior, the effective porosity was precisely linked to the corresponding pore volume change and the degree of deformation (compressive strain). Consequently, a general equation correlating the effective porosity, ε_c (Eq. 4) as a function of compressive strain (s_{TR}) and uncompressed porosity (ε_o) was derived and implemented into the main framework to calibrate the non-dimensional effective pore size parameter, $(k/\varepsilon)^{0.5}$ given in the traditional Leverett approach (Eq. 1).

$$s_{TR} = -0.0083\cdot C^2 + 0.0911\cdot C \qquad [3]$$

$$\varepsilon_c = \left[\frac{0.9}{1+s_{TR}} + 0.1\right]\cdot\varepsilon_o \qquad [4]$$

Recognizing the fact that the surface tension of water is sensitive to the temperature, the temperature effect was imposed through the previously given equation of the surface tension of water as a function of temperature. Furthermore, the temperature sensitivity of the SGL 24 series was taken into account by introducing a tunable

parameter, $(293/T)^6$ (T, in Kelvin), which is deduced based on the generated expanded database of the tested DM samples.

$$\gamma = -1.78\times10^{-4}(T) + 0.1247 \quad [5]$$

After integration of all these representative relationships into the main framework of the traditional approach, the new form of Leverett approach appropriate for the tested *SGL 24 series DMs* (coated with MPL) is found as:

$$P_C = \underbrace{(293/T)^6 \cdot \gamma(T)\cdot}_{\text{Temperature effect}} \underbrace{2^{0.4-C}\sqrt{\frac{\varepsilon_c}{k}}\cdot}_{\text{Compression effect}} \underbrace{K(s_{nw})}_{\text{Mixed wettability}} \quad [6]$$

where C, ε_c, k, γ and T represent the compression pressure, compressed porosity, absolute permeability, surface tension and temperature, respectively. $K(s_{nw})$ represents the new form of Leverett function given in Eq. 2.

In summary, the final form of the capillary pressure equation given in Eq. 6 is composed of three main terms. The first term $(293/T)^6 \cdot \gamma$ (T) accounts for the effect of temperature. The corresponding change in surface tension is included in the analytical framework through both the surface tension term and the tunable parameter, $(293/T)^6$, deduced from broad set of experimental data. The second term, $2^{0.4-C}$ $(\varepsilon_c/k)^{0.5}$, embodies the effect of compression on the morphological characteristics of the fuel cell DM. The final term is the new Leverett type function $K(s_{nw})$ that incorporates the effects of mixed wettability characteristics of the tested DM samples and the amount of PTFE loading in the DM.

Validation and Limitations: Figures 5 depicts the comparison of capillary pressures predictions by the present and the standard Leverett approach with the experimental data of SGL 24DC carbon paper at 1.4 MPa compression. As seen from Fig. 5, the present approach (Eq. 6) successfully predicts the capillary pressure, however exhibits small deviations in the saturation range of 0.50 to 0.70. This deviation likely stems from the complex shape of the capillary pressure-saturation curves. However, at high saturations (s_{nw}>0.70), the new approach successfully captures the change in capillary pressure, predicting the measured capillary pressure within an uncertainty of ±12% of the measured value over the entire saturation domain ($0<s_{nw}<1$). In contrast, the standard Leverett approach deviates enormously, nearly up to two orders of magnitude from the experimental data over the entire saturation domain, especially at high saturations (s_{nw}>0.5).

In terms of limitations, it is important to emphasize that the final form of the present empirical equation given in Eq. 6 is deduced from the capillary pressure-saturation measurements of SGL 24 series carbon paper including: SGL 24BC (5% PTFE of *wt*.), SGL 24CC (10% PTFE of *wt*.) and SGL 24DC (20% PTFE of *wt*.). Therefore the present approach is applicable for the tested DM samples within the limits of testing conditions. For developing a more generalized approach, additional benchmarking of

different DM samples needs to be performed to expand the database. Our lab is currently working on expanding this database and will report in subsequent publications.

One final note, the present correlation given in Eq. 6 is derived based on the generated data for the DM samples coated with micro-porous layer. Therefore, the porous media of interest herein is a composite structure. The capillary pressure-saturation curves of the DM macro-substrate (without MPL) can be extracted from the overall behavior of the composite structure by using the corresponding the pore size distribution and porosities of the macro and micro-substrate (MPL).

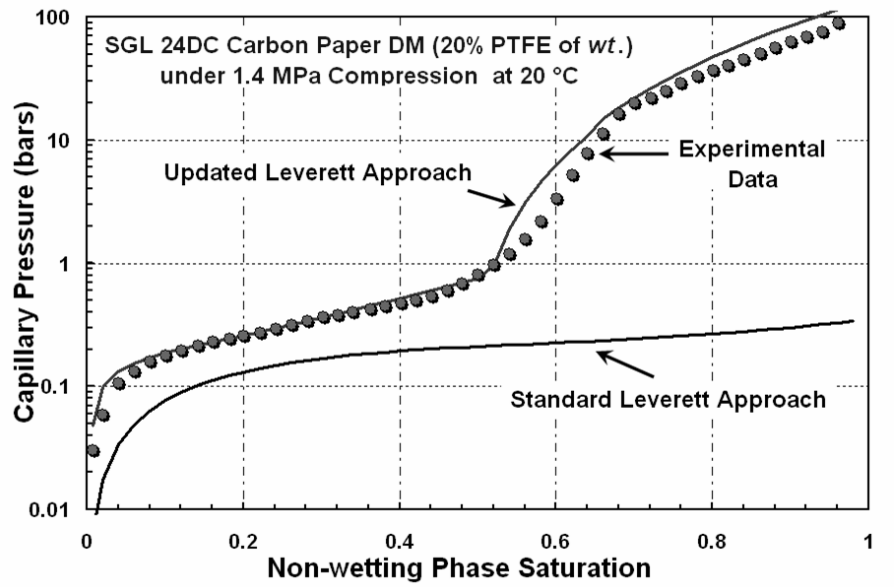

Figure 5: Comparison of the new Leverett approach (given in Eq. 6), the standard Leverett approach (Eq. 1) and the experimental data for SGL 24DC (20% PTFE) under 1.4 MPa compression.

Conclusions

Direct experimental capillary pressure-saturation data for SGL 24 series DMs (coated with MPL) are generated to develop a validated capillary pressure-saturation correlation that enables precise description of the capillary transport in these materials tailored with mixed wettability. The key features of the present approach are: *i*) the present approach embodies the non-uniform wettability characteristics of the fuel cell DM, thereby accounting for the variations in transport parameters with full spatial anisotropy of the DM, *ii*) it accounts for the variations in internal contact angle caused by the non-uniform wettability characteristics, therefore eliminates the need for the selection of a single surface contact angle, and finally *iii*) it incorporates the effects of compression and temperature on the capillary transport characteristics of the tested DM samples and performs the necessary adjustments to predict the capillary pressure as a function of hydrophobic additive content, compression pressure, uncompressed porosity and temperature. This improved approach will help to close the loop between the modeling studies and missing transport relationships for fuel cell porous media.

Acknowledgments

This research is supported by National Science Foundation under the Grant # CTS-0414319.

References

1. M. F. Mathias, J. Roth, J. Fleming, and W. Lehnert, in *Handbook of Fuel Cells–Fundamentals, Technology and Applications*, W. Lietsich, A. Laman, and H. A. Gasteiger, Editors, vol. 3, p. 517, John Wiley & Sons, New York (2003).
2. E. C. Kumbur, K. V. Sharp, and M. M. Mench, *J. Power Sources*, **168**, 356 (2007).
3. J. H. Nam, and M. Kaviany, *Int. J. Heat and Mass Transfer*, **46**, 4595, (2003).
4. N. Djilali, *Energy*, **32**, 269 (2007).
5. M. C. Leverett, *American Inst. Mining and Metallurgical Engineers -Petroleum Development and Technology*, **142**, 152 (1941).
6. H. Ohn, T. V. Nguyen, D. Jacobson, D. Hussey, and M. Arid, *ECS Transactions*, **1 (6)**, 481 (2006).
7. E. C. Kumbur, K. V. Sharp, and M. M. Mench, *J. Electrochem. Soc*., in review (Part 1) (2007).
8. E. C. Kumbur, K. V. Sharp, and M. M. Mench, *J. Electrochem. Soc*., in review (Part 2) (2007).
9. E. C. Kumbur, K. V. Sharp, and M. M. Mench, *J. Electrochem. Soc*., in review (Part 3) (2007).
10. Y. M. Volfkovich, V. S. Bagotzky, V. E. Sosenkin, and I. A. Blinov, *Colloids and Surfaces A*: *Physicochemical and Engineering Aspects*, **187-188**, 349 (2001).
11. E. C. Kumbur, K. V. Sharp, and M. M. Mench, *J. Power Sources*, **140**, 333 (2006).
12. J. Bachmann, and R. R. Van Der Ploeg, *J. Plant Nutrition Soil Science*, **165**, 468 (2002).
13. A. Dominguez, H. Perez-Aguilar, F. Rojas, and I. Kornhauser, *Colloids and Surfaces A*: *Physicochemical and Engineering Aspects*, **187-188**, 415 (2001).
14. N. M., Okusu, and K. S. Udell, *ASME*: *Fluids Engineering Division*, **82**, 13 (1989)
15. A. Bazylak, D. Sinton, Z.-S. Liu, and N. Djilali, *Journal of Power Sources*, **163**, 784-792 (2007).